J Wood Sci (2000) 46:109–114

ORIGINAL ARTICLE

Ugai Watanabe · Misato Norimoto · Toshiro Morooka

Cell wall thickness and tangential Young's modulus in coniferous early wood

Received: February 22, 1999 / Accepted: June 28, 1999

Abstract To investigate the effect of wall thickening around cell corners on the tangential Young's modulus of coniferous early wood, tapered beam cell models in which the variation of the cell wall thickness in the axial direction was taken into account were constructed for seven species. Their tangential Young's moduli were compared with the experimental results. The calculated Young's moduli of tapered beam cell models were larger than those of the models composed of the cell walls with uniform thickness, although both models showed almost the same density. For some species the calculated Young's moduli of the models in which the cell wall thickness increased curvilinearly in the axial direction were much closer to the experimental values. The reduction of the radial cell wall deflection due to the increase of the stiffness around cell corners was considered to increase the tangential Young's modulus of a wood cell.

Key words Tangential Young's modulus · Wood cell model · Cell wall thickness · Cell corner

Introduction

In previous articles[1,2] the relation between the tangential Young's moduli and the transverse cell shapes for seven kinds of coniferous early wood was investigated using cell models constructed by power spectrum analysis. The calculated Young's moduli of the cell models explained qualitatively the change of the experimental Young's moduli with density and the difference in the experimental values among species. However, the calculated values were lower than the experimental values for all species examined. Two reasons may be considered for the lower calculated values of the tangential Young's modulus of the cell model: the validity of the axial and bending Young's moduli of the wood cell wall in the perimetric direction and the variation of the cell wall thickness in the perimetric direction.

The axial and bending Young's moduli were calculated as 14.3 and 15.6 GPa, respectively, in previous articles.[1,2] If these two values are about 20.0 GPa, the calculated Young's moduli become larger and closer to the experimental results. However, this value cannot be obtained from a cell wall model constructed with reference to a standard wood cell wall structure.[1–6] Therefore, the two values for Young's moduli of the cell wall cannot be the main reason for the lower calculated values of the tangential Young's modulus of the cell model.

The cell models described in the previous articles were constructed using cell walls with uniform thickness in the perimetric direction. In reality, the cell wall thickness is not uniform, being somewhat thicker around cell corners. Taking into account the effects of beam thickness on stiffness, it is estimated that the thickening of the cell walls around cell corners contributes to an increase in transverse Young's modulus of a wood cell. The variation of the cell wall thickness in the perimetric direction may become an important factor when analyzing the mechanical behavior of a wood cell.

In this study we derived an equation to calculate the tangential Young's modulus of a tapered beam cell model in which the cell wall thickness varied in the axial direction. Furthermore, two types of tapered beam cell model were constructed for the species used in the previous articles, and their tangential Young's moduli were compared with the experimental values to investigate the effects of tapered cell walls on the tangential Young's modulus of coniferous early woods.

U. Watanabe (✉) · M. Norimoto · T. Morooka
Laboratory of Property Enhancement, Wood Research Institute, Kyoto University, Uji, Kyoto 611-0011, Japan
Tel. +81-774-38-3655 or +81-774-38-3658; Fax +81-774-38-3600
e-mail: uwatanab@kuwri.kyoto-u.ac.jp

This report was presented at the 49th annual meeting of the Japan Wood Research Society, Tokyo, April 1999

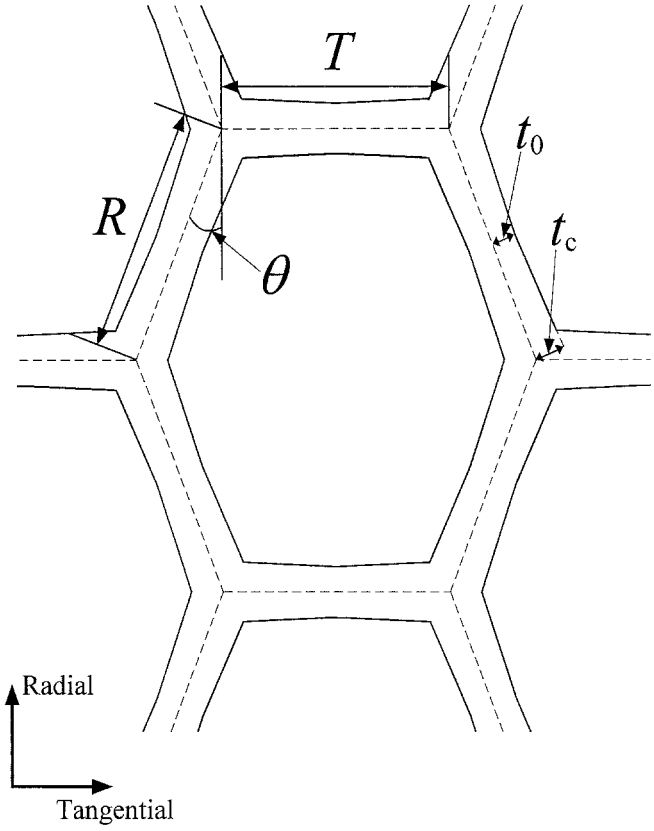

Fig. 1. Transverse shape of A-model. R, axial length of the radial cell wall; T, axial length of the tangential cell wall; θ, element angle; t_0, half of the cell wall thickness at the central portion; t_c, half of the cell wall thickness at the cell corner

Tangential Young's modulus of a tapered beam cell model

Figure 1 shows a tapered beam cell model and its geometric parameters. R and T show the axial length of radial cell wall and that of tangential cell wall, t_0 and t_c show the cell wall thickness in the central portion and that at cell corner, and θ shows the element angle, respectively. When this model is loaded in the tangential direction, the radial cell walls bend, and all of the cell walls deform in the axial direction.[7] The deflection of the radial cell wall δ is given by

$$\begin{aligned} \overline{W}\delta\cos\theta &= 2\int_0^{\frac{R}{2}} \frac{1}{E_b I(x)} Wx\cos\theta \cdot \overline{W}x\cos\theta dx \\ \overline{W}\delta &= \frac{2W\overline{W}\cos\theta}{E_b}\int_0^{\frac{R}{2}} \frac{x^2}{I(x)}dx \end{aligned} \tag{1}$$

where W, $\overline{W}$, E_b, and $I(x)$ are a force acting in the tangential direction, the virtual force, the bending Young's modulus of the cell wall, and the second moment of inertia of the cell wall, respectively. Substituting $\overline{W} = 1$ for Eq. (1) gives

$$\delta = \frac{3W\cos\theta}{bE_b}\int_0^{\frac{R}{2}} \frac{x^2}{\left\{t_R(x)\right\}^3}dx \tag{2}$$

where b is the cell wall depth, and $t_R(x)$ is a function expressing the variation of the radial cell wall thickness along the axial direction. The expression $2t_R(x)$ is equal to the radial cell wall thickness at x. The tangential strain of the cell model caused by the radial cell wall deflection ε_b can be derived as

$$\begin{aligned} \varepsilon_b &= \frac{\delta\cos\theta}{T + R\sin\theta} \\ &= \frac{3W\cos^2\theta}{bE_b(T + R\sin\theta)}\int_0^{\frac{R}{2}} \frac{x^2}{\left\{t_R(x)\right\}^3}dx \\ &= \frac{3\sigma_T\cos^3\theta}{E_b(T + R\sin\theta)}\int_0^{\frac{R}{2}} \frac{x^2}{\left\{t_R(x)\right\}^3}dx \end{aligned} \tag{3}$$

where σ_T is the stress in the tangential direction.

The axial displacements of the radial and tangential cell walls, $\varepsilon_a^R R\sin\theta$ and $\varepsilon_a^T T$, respectively, are

$$\varepsilon_a^R R\sin\theta = \frac{W\sin^2\theta}{bE_a}\int_0^{\frac{R}{2}} \frac{1}{t_R(x)}dx \tag{4a}$$

$$\varepsilon_a^T T = \frac{2W}{bE_a}\int_0^{\frac{T}{2}} \frac{1}{t_T(x)}dx \tag{4b}$$

where ε_a^R and ε_a^T are the axial strain of the radial and the tangential cell walls, respectively, E_a is the axial Young's modulus of the cell wall, and $t_T(x)$ is a function expressing the variation of the tangential cell wall thickness in the axial direction. The expression $2t_T(x)$ is equal to the tangential cell wall thickness at x. The tangential strain of the cell model caused by the axial deformation of the cell walls ε_a can be derived as

$$\begin{aligned} \varepsilon_a &= \frac{\varepsilon_a^T T + \varepsilon_a^R R\sin\theta}{T + R\sin\theta} \\ &= \frac{\sigma_T R\cos\theta}{E_a(T + R\sin\theta)}\left\{\sin^2\theta\int_0^{\frac{R}{2}} \frac{1}{t_R(x)}dx + 2\int_0^{\frac{T}{2}} \frac{1}{t_T(x)}dx\right\} \end{aligned} \tag{5}$$

All strain of tapered beam cell model is the sum of Eqs. (3) and (5). Therefore, the tangential Young's modulus of the cell model E_T is given by

$$\begin{aligned} \frac{1}{E_T} = \frac{R\cos\theta}{T + R\sin\theta}\Bigg[&\frac{3\cos^2\theta}{E_b}\int_0^{\frac{R}{2}} \frac{x^2}{\left\{t_R(x)\right\}^3}dx \\ &+ \frac{1}{E_a}\left\{\sin^2\theta\int_0^{\frac{R}{2}} \frac{1}{t_R(x)}dx + 2\int_0^{\frac{T}{2}} \frac{1}{t_T(x)}dx\right\}\Bigg] \end{aligned} \tag{6}$$

Tangential Young's modulus of A-model

As a simple case, an equation for E_T of a tapered beam cell model in which the cell wall thickness increased linearly

Table 1. Geometric parameters of A-models for seven species

Species	R (μm)	T (μm)	θ (°)	t_0 (μm)	t_c (μm)	t (μm)
Cryptomeria japonica	26.4	19.1	17	0.99	1.21	2.20
Chamaecyparis obtusa	20.0	18.7	21	2.03	2.48	4.50
Picea glehnii	20.2	23.0	13	1.58	1.93	3.50
Pinus densiflora	25.1	31.0	12	2.39	2.92	5.30
Pinus radiata	25.6	28.0	18	2.48	3.03	5.50
Metasequoia glyptostroboides	28.7	33.1	10	1.26	1.54	2.80
Tsuga heterophylla	22.2	34.2	6	1.80	2.20	4.00

R, axial length of the radial cell wall; T, axial length of the tangential cell wall; θ, element angle; t_0, half of the cell wall thickness at the central portion; t_c, half of the cell wall thickness at the cell corner; t, cell wall thickness of S-model[1,2]

from $2t_0$ to $2t_c$ ($t_0 < t_c$) in the axial direction, as shown in Fig. 1, was obtained as follows:

$$\frac{1}{E_T} = \frac{\cos\theta}{(T/R + \sin\theta)(t_c - t_0)}\left[\frac{1}{E_a}\left(\frac{R\sin^2\theta}{2} + T\right)\times \log\frac{t_c}{t_0} + \frac{3R^3\cos^2\theta}{8(t_c - t_0)^2 E_b}\times \left\{\log\frac{t_c}{t_0} + \frac{4t_0(t_c - t_0) + 3t_0^2}{2t_c^2} - \frac{3}{2}\right\}\right] \quad (7)$$

Hereafter, the cell model in Fig. 1 is referred to as A-model. E_Ts of A-models for seven species (*Chamaecyparis obtusa* Endl., *Cryptomeria japonica* D. Don, *Metasequoia glyptostroboides* Hu et Cheng, *Picea glehnii* Mast., *Pinus densiflora* Sieb. et Zucc., *Pinus radiata* D. Don, *Tsuga heterophylla* Sarg.) were calculated using the geometric parameters shown in Table 1.[1,2] The parameters t_0 and t_c were determined by two requirements: the relation of

$$\frac{t_c - t_0}{t} = 0.1 \quad (8)$$

where t is the cell wall thickness of the models constructed in the previous articles[1,2] (hereafter that model is referred to as S-model), and that the A-models showed the same density values as those of the S-models. The deflection of laminates such as the wood cell walls significantly depends on the volume fractions and mechanical properties of the outer layers. Therefore, the elastic modulus of the cell wall calculated using the lamination theory[8] is considered to be proper for E_b. Regarding the mechanical property of the cell wall as uniform along the axial direction, the values of 14.3 and 15.6 GPa were used for E_a and E_b, respectively.[1,2]

Tangential Young's modulus of B-model

The thickness of real wood cell wall increases curvilinearly from the central portion of the cell wall to the cell corner, as shown in Fig. 2. An equation for E_T of a tapered beam cell model in which this cell wall shape was taken into account,

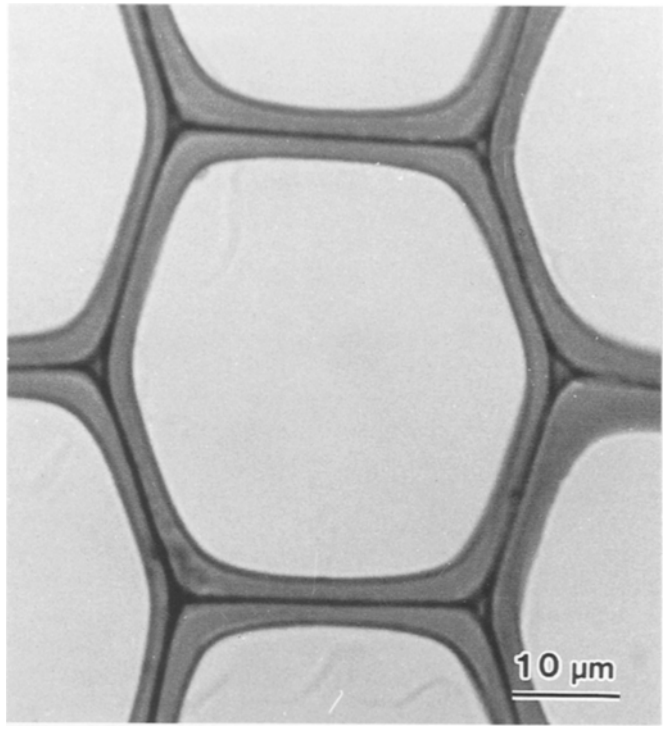

Fig. 2. Transverse cell shape of *Pinus densiflora*

as shown in Fig. 3, was derived. The following equations were adopted for $t_R(x)$ and $t_T(x)$.

$$t_{R,T}(x) = \alpha + m\left(\frac{\beta_{R,T}}{\beta_{R,T} - x}\right) \quad (9)$$

Hereafter, the cell model in Fig. 3 is called B-model. Substituting Eq. (9) for Eq. (6), the E_T of B-model is given by

$$\frac{1}{E_T} = \frac{R\cos\theta}{T + R\sin\theta}\left[\frac{3\cos^2\theta}{E_b}\int_0^{\frac{R}{2}}\frac{x^2(\beta_R - x)^3}{\{\alpha(\beta_R - x) + m\beta_R\}^3}dx + \frac{1}{E_a}\left\{\sin^2\theta\int_0^{\frac{R}{2}}\frac{\beta_R - x}{\alpha(\beta_R - x) + m\beta_R}dx + 2\int_0^{\frac{T}{2}}\frac{\beta_T - x}{\alpha(\beta_T - x) + m\beta_T}dx\right\}\right] \quad (10)$$

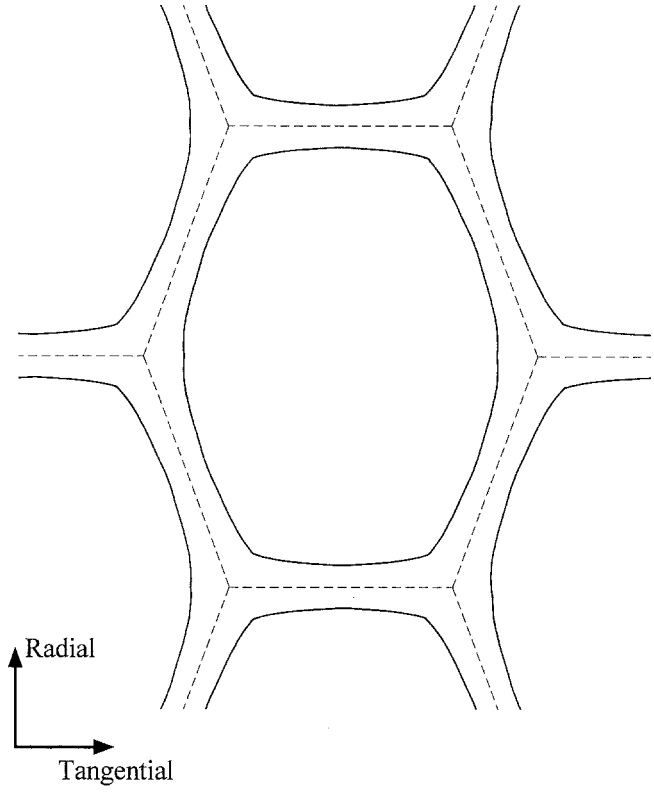

Fig. 3. Transverse shape of B-model

Table 2. Coefficients of $t_R(x)$ and $t_T(x)$ for seven species

Species	α	β_R	β_T	m
Cryptomeria japonica	0.20	18.0	13.0	0.50
Chamaecyparis obtusa	1.20	12.2	11.4	0.50
Picea glehnii	0.85	13.9	15.7	0.50
Pinus densiflora	1.60	15.3	18.9	0.50
Pinus radiata	1.65	15.2	16.6	0.50
Metasequoia glyptostroboides	0.50	19.6	22.6	0.50
Tsuga heterophylla	1.00	13.9	21.5	0.50

Table 2 shows coefficient values of α, β_R, β_T, and m for calculating the E_Ts of B-models for seven species. The densities of B-models calculated from these coefficients were almost the same as those of S-models. The values of 14.3 and 15.6 GPa were used for E_a and E_b.[1,2]

Finite-element analysis of deflection and axial deformation of tapered cell walls

The deflection and axial deformation of tapered cell walls used in A-models and B-models for seven species were investigated using a p-version finite-element analysis program (StressCheck V4.0; Engineering Software Research & Development.) and compared with those obtained from Eqs. (2) and (4). Figure 4 shows an element division of the tapered cell wall used in this analysis. X and Y indicate the axial and thickness directions of the cell wall, respectively.

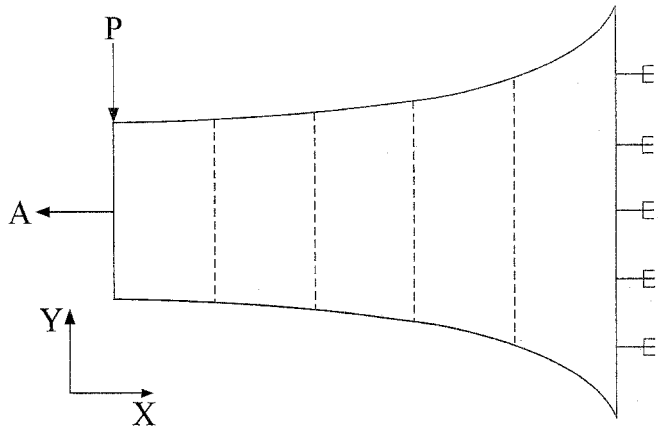

Fig. 4. Element division of tapered cell wall for p-version finite-element analysis. *X*, axial direction; *Y*, thickness direction; *P*, point force; *A*, axial force

All of the tapered cell walls examined were divided into five equal parts in the X direction. The cell wall was completely constrained at the end with the largest thickness (the right end in Fig. 4), and a point force in Y direction or an axial force in X direction was applied at the opposite end. A value of 14.3 GPa was used for the Young's modulus E in this analysis. For Poisson's ratio, a value of 0.3 was used. Furthermore, the E_Ts of A-models and B-models based on the results of finite-element analyses were calculated and compared with those obtained by Eqs. (7) and (10).

Comparison of experimental and calculated values of tangential Young's modulus

Figure 5 shows the relation between densities and experimental Young's moduli and the calculated moduli of A-models and S-models for seven species. The difference was within 3.8% between cell wall deflections of A-models calculated from Eq. (2) and those obtained from finite-element analyses. For axial displacement, the difference was within 1.7% between the values calculated from Eq. (4) and those obtained from finite-element analyses. The E_Ts of A-models for seven species are represented by the values calculated by Eq. (7), as they are almost the same as the results obtained by finite-element analyses. For all species examined, the E_T of the A-model was larger than that of the S-model, although both models showed the same density. The E_T of S-model can be given by the following equation.[1,2,7]

$$\frac{1}{E_T} = \frac{\cos\theta\left(2T/R + \sin^2\theta\right)}{(t/R)(T/R + \sin\theta)E_a} + \frac{\cos^3\theta}{(t/R)^3(T/R + \sin\theta)E_b} \tag{11}$$

The first terms of Eqs. (7) and (11), A' and A, express the axial contribution; and the second terms, B' and B, express the bending contribution, respectively. A'/A and B'/B were calculated for seven species to investigate the effect of the tapered cell walls on the deformation of cells. Results are

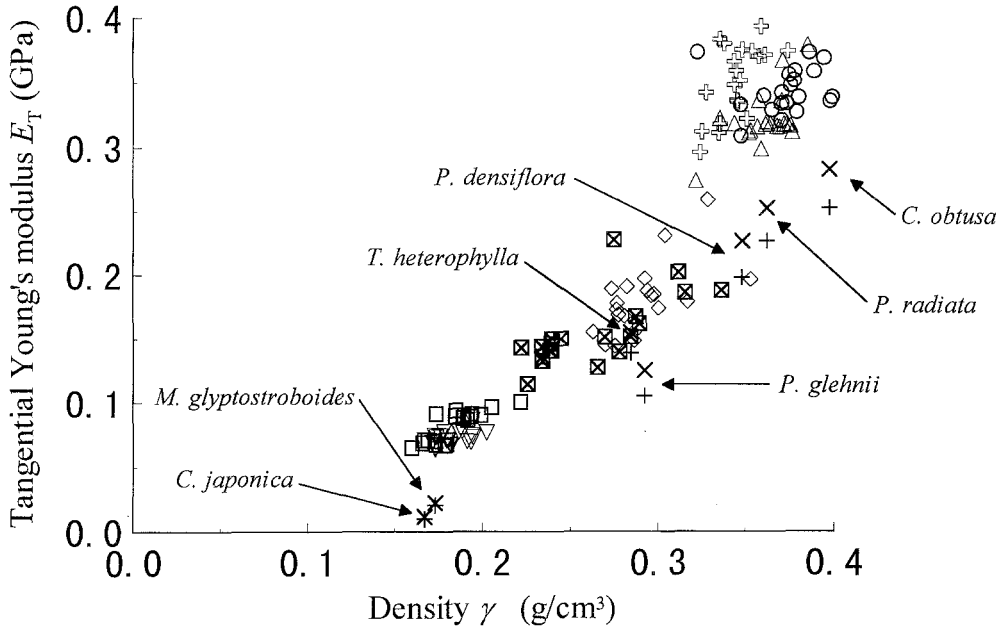

Fig. 5. Comparison of experimental and calculated values of tangential Young's modulus. *Squares, Cryptomeria japonica; circles, Chamaecyparis obtusa; diamonds, Picea glehnii; open crosses, Pinus densiflora; triangles, Pinus radiata; inverted triangles, Metasequoia glyptostroboides; squares with ×, Tsuga heterophylla; plus sign*, calculated value of S-model; ×, calculated value of A-model

Table 3. Calculated values of A'/A and B'/B for seven species

Species	A'/A	B'/B
Cryptomeria japonica	1.00	0.87
Chamaecyparis obtusa	1.00	0.87
Picea glehnii	1.00	0.87
Pinus densiflora	1.00	0.87
Pinus radiata	1.00	0.87
Metasequoia glyptostroboides	1.00	0.87
Tsuga heterophylla	1.00	0.87

A'/A, ratio of the first term of Eq. (7) to that of Eq. (11); B'/B, ratio of the second term of Eq. (7) to that of Eq. (11)

Table 4. Half of the cell wall thickness of B-models for seven species calculated from Eq. (9)

Species	t_0 (μm)	t_c (μm)	
		Radial wall	Tangential wall
Cryptomeria japonica	0.70	2.16	2.11
Chamaecyparis obtusa	1.70	3.97	4.05
Picea glehnii	1.35	2.68	2.71
Pinus densiflora	2.10	4.43	4.38
Pinus radiata	2.15	4.82	4.84
Metasequoia glyptostroboides	1.00	2.38	2.35
Tsuga heterophylla	1.50	3.48	3.44

t_0, half of the cell wall thickness at the central portion; t_c, half of the cell wall thickness at the cell corner

Table 5. Calculated results of A''/A and B''/B for seven species

Species	A''/A	B''/B_{Cal}	B''/B_{FE}
Cryptomeria japonica	1.09	0.69	0.68
Chamaecyparis obtusa	1.05	0.74	0.79
Picea glehnii	1.04	0.74	0.79
Pinus densiflora	1.04	0.75	0.83
Pinus radiata	1.04	0.75	0.82
Metasequoia glyptostroboides	1.06	0.70	0.69
Tsuga heterophylla	1.05	0.72	0.74

A''/A, ratio of the first term of Eq. (10) to that of Eq. (11); B''/B, ratio of the second term of Eq. (10) to that of Eq. (11); Cal, calculated from Eqs. (10) and (11); FE, calculated by finite-element analysis

shown in Table 3. Because A'/A shows a value of about 1.0 for all species, the axial contribution is not influenced by the change from the straight cell walls to the tapered ones. On the other hand, B'/B shows a value below 1.0 for all species. These results indicate that a smaller deflection of the tapered cell wall increases E_T of cell models.

Figure 6 shows the relation between densities and experimental Young's moduli as well as calculated moduli of B-models, A-models, and S-models for seven species. The difference was 3.4%–10.0% between cell wall deflections of B-models calculated from Eq. (2) and those obtained from finite-element analyses. For axial displacement, the difference was within 1.9% between the values calculated from Eq. (4) and those obtained from finite-element analyses. Therefore, the E_T of the B-model calculated from Eq. (10) and that obtained from finite-element analyses are indicated in Fig. 6 for each species. For all species examined, the E_T of the B-model was the largest among the three cell models although densities were of almost the same value. The values of *Chamaecyparis, obtusa, Pinus radiata, Picea glehnii*, and *Tsuga heterophylla* became considerably closer to their experimental values. The t_0 and t_c values of B-models calculated by Eq. (9) are shown in Table 4. The t_0 value of the B-model was smaller than that of the A-model and the $t/2$ for each species. Table 5 shows the calculated results of A''/A and B''/B for each species where A'' and B'' express the first and second terms of Eq. (10), respectively. The value of A''/A was slightly larger than that of A'/A for all species. However, this increase may not significantly influence the deformation of a cell because A is a smaller

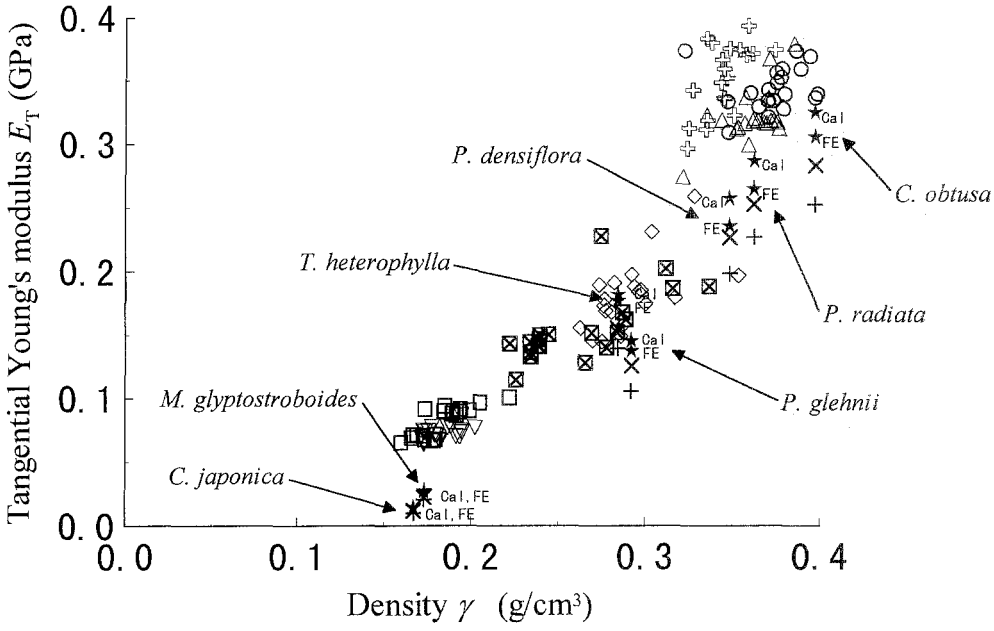

Fig. 6. Comparison of experimental and calculated values of tangential Young's modulus. *Stars*, calculated value of B-model; *Cal*, calculated from Eq. (10); *FE*, calculated by finite-element analysis. See Fig. 5 for explanation of other symbols

value than B.[1,2] On the other hand, the value of B''/B was smaller than that of B'/B for all species; that is, the cell wall deflection of the B-model decreased compared with that of the A-model although t_0 of the B-model was a smaller value. From these results, it is considered that the larger values of E_T of the B-models are mainly attributed to the decrease in cell wall deflection.

When a wood cell is loaded in the tangential direction, the radial cell walls deflect owing to the displacement of cell corners. The wall thickening around cell corners increases the stiffness and reduces the displacement, resulting in a reduction of bending deflection of whole radial walls. At the same time, the cell walls deform in the axial direction. However, the axial contribution to cell deformation is negligible because the whole strain of a cell by this deformation is much smaller and the wall thickening around cell corners does not influence significantly the axial deformation of the cell wall. Therefore, in coniferous early woods, the effect of the large stiffness around cell corners on the bending property of the radial cell wall is considered to relate strongly to the larger experimental value of tangential Young's modulus than the calculated value of the S-model. These considerations suggest that the wall thickness around cell corners as well as transverse cell shapes are important factors in the mechanical properties on the transverse plane in wood.

References

1. Watanabe U (1998) Shrinking and elastic properties of coniferous wood in relation to cellular structutre. Wood Res 85:1–47
2. Watanabe U, Norimoto M, Ohgama T, Fujita M (1999) Tangential Young's modulus of coniferous early wood investigated using cell models. Holzforschung 53:209–214
3. Schniewind AP (1972) Elastic behavior of the wood fiber. In: Jayne BA (ed) Theory and design of wood and fiber composite materials. Syracuse University Press, New York, pp 83–95
4. Chou PC, Carleone J, Hsu CM (1972) Elastic constants of layered media. J Comp Mater 6:80–93
5. Ohgama T, Norimoto M (1984) Elastic constants of wood cell wall. Bull Fac Educ Chiba Univ 33:127–145
6. Saiki H (1970) Proportion of component layers in tracheid wall of early and late wood of some conifers (in Japanese). Mokuzai Gakkaishi 16:244–249
7. Gibson LJ, Ashby MF (1988) The mechanics of honeycombs. In: Cellular solids. Pergamon Press, Oxford, pp 69–118
8. Jones RM (1975) Macromechanical behavior of a laminate. In: Mechanics of composite materials (international student edition). McGraw-Hill Kogakusha, Tokyo, pp 147–237